Journal of the Brazilian Society of Mechanical Sciences and Engineering (2022) 44:147
https://doi.org/10.1007/s40430-022-03410-4

REVIEW PAPER

Reducing the discretization error for a poroelasticity problem in variables having extreme values

Sandro Rodrigues[1,2] · Márcio Augusto Villela Pinto[3] · Márcio André Martins[1] · Sebastião Romero Franco[4]

Received: 20 July 2021 / Accepted: 4 February 2022

Abstract
In this work, we aim to reduce and estimate the numerical error using Repeated Richardson extrapolation (RRE), which is characterized as a post-processing method of low computational cost based on the Richardson series. This study considers variables with extreme values, corresponding to the flow problem in a deformable porous medium. We employed the Finite Difference Method with second-order spatial approximations, Dirichlet and Neumann boundary conditions, and temporal approximation using the Crank–Nicolson method, thus generating large systems of equations, which are solved by employing the multigrid method with the Vanka smoother. We used the RRE procedure considering the solutions in 11 grids with different spacings. However, we verified in this case that the direct application of RRE to variables with extreme values was not efficient, according to behavior described in the literature. So, we used a methodology that involving polynomial interpolation and optimization method. The results obtained indicate that the methodology used in this study is promising in terms of reducing the discretization error and increasing the accuracy of numerical solutions, as well as obtaining reliable and accurate estimates.

Keywords Richardson extrapolation · Poroelasticity · Discretization error · Error estimator

1 Introduction

In Computational Fluid Dynamics (CFD), the accuracy of numerical solutions represents a great challenge for researchers. Therefore, extrapolation methods have been increasingly used as effective computational tools and have gained notoriety in this environment. An extrapolation method will be considered adequate if it takes into account the asymptotic behavior of a convergent sequence [38]. One of the best-known techniques is Richardson extrapolation (RE). By applying RE recursively, it is possible to enhance its effectiveness. This process is called Repeated Richardson extrapolation (RRE) [9].

The first application of RRE was presented in the work of Richardson and Gaunt [35] that considered two levels of extrapolation and applied this technique to equations in integral form, such as the Volterra equation, and differential form, such as the derivatives in the Leibnitz Theorem. Applications with only two levels of RE are also found in [1, 11, 34] and result in a significant increase in the order of accuracy of numerical solutions. The use of RE with more than two extrapolation levels is observed in [21, 25, 26, 36], studies that aimed to reduce the discretization error. In addition to reducing this error, estimators are proposed in [27, 28] and applied to problems such as those described by Poisson 1D, Laplace 2D, Burgers 2D, and Navier-Stokes 2D equations.

Poroelasticity equations mathematically model the interaction between the deformation of a porous elastic material and the flow of a fluid within it. Its general three-dimensional theory was formulated by Biot, [5, 6]. The analysis

Technical Editor: Daniel Onofre de Almeida Cruz.

✉ Sandro Rodrigues
srodrigues@unicentro.br

Márcio Augusto Villela Pinto
marcio_villela@ufpr.br

Márcio André Martins
mandre@unicentro.br

Sebastião Romero Franco
romero@unicentro.br

[1] Department of Mathematics, State University of Centro-Oeste, Guarapuava, Brazil

[2] Graduate Program in Numerical Methods in Engineering, Federal University of Paraná, Curitiba, Brazil

[3] Department of Mechanical Engineering, Federal University of Paraná, Curitiba, Brazil

[4] Department of Mathematics, State University of Centro-Oeste, Irati, Brazil

Published online: 19 March 2022

and numerical simulation of the Biot model have become more popular and more discussed due to its range of applications in Medicine, Petroleum Engineering, Biomechanics, and other fields of Science and Engineering, [10, 18]. This is a typical mathematical model of coupled differential equations, whose numerical verification requires special attention and is not particularly consolidated in the literature.

The mathematical model we used in this work is represented by the system of equations that describes the Biot consolidation problem for a saturated, homogeneous, and isotropic porous medium, filled by a single incompressible fluid, [15, 19]. The equations are discretized by using the Finite Difference Method (FDM) with second-order accuracy spatial approximations, as well as Dirichlet and Neumann boundary conditions. For temporal approximation, we used the Crank–Nicolson method, thus generating large systems of linear equations that are solved by the multigrid method with the Vanka smoother, [15, 41]. Multigrid methods are commonly used to solve large linear systems [7, 40, 42], particularly in poroelasticity problems [2, 18, 23, 43] or general problems [3, 14, 22, 24, 32, 33].

In this work, we analyzed the following variables of interest: maximum displacement ($u_{\max}$) and maximum pressure ($p_{\max}$). These variables may lead to complications in the use of RRE, as described in the literature, [27, 31]. These complications can occur due to the change in the coordinate location of the variable of interest in different grids. Therefore, considering that the study of variables of this nature is frequent in CFD, further investigations in this area are necessary.

The results obtained in this study indicate that the proposed methodology is promising in the sense of increasing the accuracy of numerical solutions and the accuracy and reliability of the Richardson estimator for the poroelasticity problem. The remainder of this paper is organized as follows: in Sect. 2, we present the mathematical and numerical models; in Sect. 3, we explain the theoretical foundation necessary for the comprehension of this paper; in Sect. 4, we describe the types of variables based on the grid refinement process; in Sect. 5, we show the results, and finally, in Sect. 6, we present the conclusions.

2 Mathematical and numerical models

Consider Biot's consolidation problem for a saturated, homogeneous, isotropic porous medium, filled with a single incompressible fluid following the models described in [15, 20]. By taking the one-dimensional case and considering the spatial domain $\Omega = \left(0, \frac{1}{2}\right)$ and temporal domain $(0, T]$, we have

$$\begin{cases} -\dfrac{\partial}{\partial x}\left(E\dfrac{\partial u}{\partial x}\right) + \alpha\dfrac{\partial p}{\partial x} = \mathit{U} \\ \dfrac{1}{\beta}\dfrac{\partial p}{\partial t} + \alpha\dfrac{\partial}{\partial t}\left(\dfrac{\partial u}{\partial x}\right) - \dfrac{\partial}{\partial x}\left(K\dfrac{\partial p}{\partial x}\right) = \mathit{P} \end{cases}, \tag{1}$$

where E is Young's modulus, K is the hydraulic conductivity, α is the Biot–Willis constant, β is Biot's modulus, U is the density of the forces applied to the body, and P is the injection or extraction forces of the fluid in the porous medium. The components $u(x, t)$ and $p(x, t)$ represent the displacement and pressure in the spatial direction x, respectively.

Boundary conditions assume a permeable (free drainage) left boundary without displacement variation and a right boundary (zero displacement) without pressure variation, that is,

$$\begin{cases} E\dfrac{\partial u}{\partial x} = 0, & \text{if} \quad x = 0, \\ p = 0, & \text{if} \quad x = 0 \end{cases} \tag{2}$$

and

$$\begin{cases} u = 0, & \text{if} \quad x = \frac{1}{2}, \\ K\dfrac{\partial p}{\partial x} = 0, & \text{if} \quad x = \frac{1}{2}. \end{cases} \tag{3}$$

Based on the method of manufactured solutions [37], when considering the analytical solution given by

$$u(x, t) = x\sin(2\pi x)e^{-t} \tag{4}$$

and

$$p(x, t) = \left(\sin(2\pi x) + \frac{8}{3}\pi x^3\right)e^{-t}, \tag{5}$$

for $x \in \Omega$ and $0 < t \leq T$. We can define the forcing terms U and P as

$$\mathit{U} = 2\pi\left(\cos(2\pi x) + 2E\pi x\sin(2\pi x) - 2E\cos(2\pi x) + 4x^2\right)e^{-t} \tag{6}$$

and

$$\mathit{P} = \left(4K\pi^2\sin(2\pi x) - \sin(2\pi x) - 2\pi x\cos(2\pi x) - 16K\pi x\right)e^{-t}. \tag{7}$$

For the numerical model, the spatial domain is discretized by the FDM, uniform grids, and Central Difference Scheme (CDS). The temporal approximation is discretized by the Crank–Nicolson method. We considered a uniform space-time grid in $\Omega \times (0, T]$ given by $G_{h,\tau} = G_h \times G_\tau$, where

$$G_h = \{x_i = ih \mid i = 1, \ldots, N + 1\} \tag{8}$$

and

$$G_\tau = \{t_j = j\tau \mid j = 0, \ldots, , M\}. \tag{9}$$

Furthermore, we used an additional stabilization parameter in the equation corresponding to the pressure, this parameter is given in [17] by $\frac{h^2}{4E}\frac{\partial \Delta p}{\partial t}$.

Considering constant K and E, $\beta \to \infty$ and $\alpha = 1$, and adding the stabilization parameter in Eq. (1), the discretization for the inner points ($i = 2, 3, \ldots, N$) is

$$\begin{cases} -E\frac{u_{i+1}^{n+1}-2u_i^{n+1}+u_{i-1}^{n+1}}{h^2} + \frac{p_{i+1}^{n+1}-p_{i-1}^{n+1}}{2h} = U_i^{n+1} \\ \frac{\frac{u_{i+1}^{n+1}-u_{i-1}^{n+1}}{2h} - \frac{u_{i+1}^{n}-u_{i-1}^{n}}{2h}}{\tau} - \frac{h^2}{4E\tau}\left[\frac{p_{i+1}^{n+1}-2p_i^{n+1}}{h^2}\right. \\ \left. + \frac{p_{i-1}^{n+1}}{h^2} - \frac{p_{i+1}^{n}-2p_i^{n}+p_{i-1}^{n}}{h^2}\right] = \frac{P_i^{n+1}+P_i^{n}}{2} + \\ \frac{K}{2}\left(\frac{p_{i+1}^{n+1}-2p_i^{n+1}+p_{i-1}^{n+1}}{h^2} + \frac{p_{i+1}^{n}-2p_i^{n}+p_{i-1}^{n}}{h^2}\right) \end{cases}, \tag{10}$$

where i, $i-1$ and $i+1$ indicate the spatial discretization, and n and $n+1$ indicate the previous and current time steps, respectively. The time step is given by $\tau = \frac{T}{M_1}$. The length of the spatial discretization is given by $h = \frac{1}{2(N+1)}$. Similar to the inner points, adaptations of these equations can be made for the contours $i = 1$ and $i = N+1$.

After the discretizations, we obtained large systems of equations, which were solved by using the multigrid method with the three-point Vanka smoother. The multigrid method is an alternative numerical technique to iteratively solve systems of equations, obtained by discretizing differential equations. Originally proposed by Fedorenko, [12], it shows that the convergence speed when using this technique is better than that obtained when applying pure iterative methods (without the use of multigrid, thus called singlegrid).

The basic principle of the multigrid method is to use a set of grids and alternate smoothing steps at each grid level as well as the approximations of these solutions in a coarser grid (with a certain coarsening ratio) through operators that transfer information from the fine grid to the immediately coarser grid (restriction operator), and then transfer information from the coarse grid to the immediately finer grid (prolongation operator), thus reducing the entire spectrum of errors (high and low frequency errors), [7, 40, 42].

3 Numerical verification

3.1 Numerical error

For a given variable of interest, the numerical error (E) is defined as the difference between the exact analytical solution (Φ) and its numerical solution (ϕ) [13], which can be caused by several sources described in [13, 29] as: truncation errors (E_T), iteration errors (E_I), and rounding errors (E_π). When E_I and E_π are minimized or even non-existent, E_T is then called a discretization error (Eh), [13]. When Eh is the only source of numerical error, it can be represented through the Taylor series by

$$\text{Eh} = E(\phi) = c_0 h^{p_0} + c_1 h^{p_1} + c_2 h^{p_2} + \cdots = \sum_{V=0}^{\infty} c_V h^{pV}, \tag{11}$$

where the coefficients $c_0, c_1, c_2, \ldots$ are real numbers and can be functions of the dependent variable and of its derivatives, but are independent of h.

The exponents $p_0, p_1, p_2, \ldots$ are the true orders of $E(\phi)$. This set is represented by $pV = \{p_0, p_1, p_2, \ldots\}$ and is composed positive integers numbers, generally following the relation $1 \le p_0 < p_1 < \ldots$, which represents an arithmetic progression. The first element of pV, p_0, is named asymptotic order of $E(\phi)$.

The analysis of p_0 *a posteriori* of the numerical solution is based on the calculation of the effective order pE, when the analytical solution is known, and on the apparent order pU, on the contrary. Their expressions are given by:

$$pE = \frac{\log\left(\frac{\text{Eh}_1}{\text{Eh}_2}\right)}{\log(r)} \tag{12}$$

and

$$pU = \frac{\log\left(\frac{\phi_2 - \phi_1}{\phi_3 - \phi_2}\right)}{\log(r)}, \tag{13}$$

where ϕ_1, ϕ_2 and ϕ_3 correspond, respectively, to the numerical solutions for a variable of interest in the grids Ω^{h_1} (coarse), Ω^{h_2} (fine) and Ω^{h_3} (superfine), Eh_i, the discretization error associated with the grid Ω^{h_i}, and r, the refinement ratio between grids.

3.2 Repeated Richardson extrapolation

Richardson's extrapolation is given by [9]:

$$\phi_\infty = \phi_{g+1} + \frac{\phi_{g+1} - \phi_g}{r^{p_0} - 1}, \tag{14}$$

where ϕ_∞ is the estimated analytical solution, ϕ_{g+1} and ϕ_g are the numerical solutions in the fine grids $\Omega^{h_{g+1}}$ and coarse grids Ω^{h_g}, and $r = \frac{h_g}{h_{g+1}}$ is the refinement ratio. This expression is going to be effective when ϕ_g contains only discretization errors.

RRE consists of the recursive application of RE to increase the accuracy level of numerical solutions. The recursion process is created from Eq. (14), where m indicates

extrapolation, and g indicates grid levels. Eq. (14) is represented in [28] by

$$\phi_{g,m} = \phi_{g,m-1} + \frac{\phi_{g,m-1} - \phi_{g-1,m-1}}{r^{p_{m-1}} - 1}, \tag{15}$$

with $m = 1, 2, \ldots$ and $g = m + 1, m + 2 \ldots$.

From a theoretical point of view, Eq. (15) can be repeated infinitely, however, for practical applications we must consider a limit value for $g = G$, where G is a positive integer that corresponds to the number of grids that was used. It is assumed that the use of this recursive process, Eq. (15), provides a progressive increase in the order of accuracy of Eh, [27].

An analysis of the resulting order of accuracy can be performed by considering a generalization of pE and pU for RRE, as found in [25]:

$$(pE)_{g,m} = \frac{\log\left(\frac{\mathrm{Eh}_{g-1,m}}{Eh_{g,m}}\right)}{\log(r)} \tag{16}$$

and

$$(pU)_{g,m} = \frac{\log\left(\frac{\phi_{g-1,m} - \phi_{g-2,m}}{\phi_{g,m} - \phi_{g-1,m}}\right)}{\log(r)}, \tag{17}$$

where $g = 2, \ldots, G$ and $m = 1, \ldots, g - 1$ for Eq. (16); and $g = 3, \ldots, G$ and $m = 1, \ldots,$ Int $((g - 3)/2)$ for Eq. (17), where Int (γ) corresponds to the integer part of the real number γ. In this perspective, when the analytical solution is unknown, not even the true orders, RRE calculation can be performed by taking into account the values of $(pU)_{g,m-1}$ instead of p_{m-1} in Eq. (15).

3.3 Discretization error estimates

When the analytical solution Φ is unknown, the discretization error cannot be calculated. So, the concept of uncertainty (U) is used. The uncertainty of a numerical solution is calculated by the difference between the estimated analytical solution (ϕ_∞) for a variable of interest and its numerical solution (ϕ), [8], that is,

$$U(\phi) = \phi_\infty - \phi. \tag{18}$$

Following we describe a few adapted estimators, taking into account the use of RRE.

3.3.1 Estimator Δ

The Δ error estimator is given by [30]:

$$U_\Delta(\phi_{G,m}) = |\phi_{G,m-1} - \phi_{G-1,m-1}|, \tag{19}$$

where $m = G - 1$ represents the last considered extrapolation level, and $m - 1$ is the level immediately before it. Therefore, $U_\Delta(\phi_{G,m})$ provides an estimate for Em associated with $\phi_{G,m}$ whereas the values of $\phi_{G,m-1}$ and $\phi_{G-1,m-1}$.

3.3.2 Corrected Richardson's estimator (U_{cpm})

Richardson's error estimator (U_{pm}) is given by, [25]:

$$U_{pm}(\phi_{g,m}) = \frac{\phi_{g,m} - \phi_{g-1,m}}{r^{p_m} - 1}, \tag{20}$$

where g represents the grid level, m the extrapolation level, and they are valid for $m = [0, G - 2]$ and $g = [m + 2, G]$ and p_m corresponds to the values of p V.

By analyzing Eq. (20), we verify that the estimator U_{pm} does not estimate the discretization error for the last extrapolation level with maximum m, that is, it works just for $\phi_M = \{\phi_{2,1}, \phi_{3,2}, \ldots, \phi_{g,g-1}, \ldots, \phi_{G,G-1}\}$. As an alternative, it is proposed in [27] the utilization of a correction factor r^{p_m}, thus, the estimator becomes

$$U_{\mathrm{cpm}}(\phi_{g,m}) = r^{p_m} U_{pm}(\phi_{g+1,m}), \tag{21}$$

where $m = g - 1$. U_{cpm} is called the corrected U_{pm} estimator.

3.3.3 Estimator ψ^*

Considering the numerical solutions for the last extrapolation level with maximum m, ϕ_M, the estimator ψ, Eq. (22), is used, taking into account the convergence ratio of ϕ_M and the estimate for Em as follows:

$$U_\psi(\phi_{g,m}) = \frac{\phi_{g,m} - \phi_{g-1,m-1}}{\psi - 1}, \tag{22}$$

where

$$\psi = (\psi_M)_g = \frac{\phi_{g-1,m-1} - \phi_{g-2,m-2}}{\phi_{g,m} - \phi_{g-1,m-1}}, \tag{23}$$

for $g = 3, \ldots, G$.

Using U_ψ will only be effective if $|\psi| > 1$, which is associated with the convergence of ϕ_M, thus reducing the magnitude of Em, [29]. A correction for Eq. (22), according to [27], is given by:

$$\psi^* = \begin{cases} \dfrac{\phi_{g,m} - \phi_{g-1,m-1}}{\phi_{g+1,m+1} - \phi_{g,m}}, & g = 2, 3, \ldots, G-1 \\ \dfrac{(\phi_{g-1,m-1} - \phi_{g-2,m-2})^2}{(\phi_{g,m} - \phi_{g-1,m-1})(\phi_{g-2,m-2} - \phi_{g-3,m-3})}, & g = G \end{cases} . \quad (24)$$

This proposition, Eq. (24), aims to obtain an estimate for the finest grid considered, Ω^{h_g}, which is not possible with Eq. (22).

Therefore, the estimate of the numerical error related to ϕ_M becomes:

$$U_{\psi^*}(\phi_{g,m}) = \frac{\phi_{g,m} - \phi_{g-1,m-1}}{\psi^* - 1}. \quad (25)$$

3.3.4 Effectiveness of an error estimate

The quality of an uncertainty U for the numerical error E can be generally assessed by measuring its effectiveness ($\theta(U)$), defined in [44] by:

$$\theta(U) = \frac{U}{E}. \quad (26)$$

In the perfect setting, the effectiveness is $\theta(U) = 1$. An uncertainty U will be considered reliable when $\theta(U) \geq 1$ and accurate when $\theta(U) \approx 1$.

4 Particularities of the numerical solutions investigated when using RRE

The use of RRE requires numerical solutions to be obtained for a specific variable of interest in a collection of different grids. In this work, the variables of interest used are variables with extreme values, pointed in the literature as limiters to the effectiveness of using RRE, [27, 31]. Figure 1 (adapted from [27]) illustrates the behavior of this type of variable in relation to the grid refining process, in which ϕ_1 with coordinates a_1, ϕ_2 with coordinates a_2 and ϕ_3 with coordinates a_3, correspond, respectively, to the numerical solutions obtained in the grids Ω^{h_1} (coarse), Ω^{h_2} (fine) and Ω^{h_3} (superfine), with constant refining ratio ($r = h_1/h_2 = h_2/h_3$).

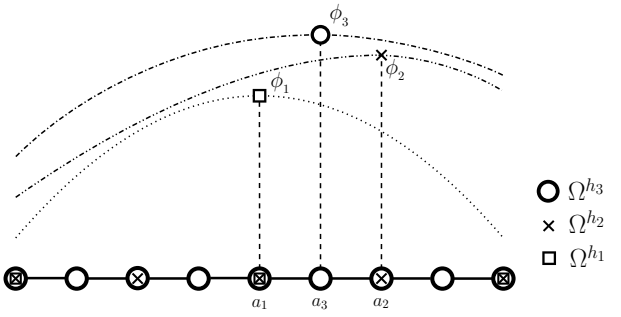

Fig. 1 Variable with an unknown location that presents alteration in its coordinates when considering different grids

For these variables, it is not possible to predetermine the coordinate location as it depends on the adopted grid, Fig. 1. In this case, the direct utilization of RRE does not imply the reduction of the numerical error because of the effect of this change in the location of ϕ in different grids, as described in [27]. The use of RRE for variables with extreme values, according to [27], must be performed in a way that the effects caused by the change in the coordinates in different grids are minimized or eliminated. From this perspective, polynomial interpolation followed by the application of optimization methods leads to results with a higher level of accuracy.

That said, we consider the $p + 1$ nodal points located in the proximities (neighborhoods) of the discrete maximum (or minimum) point, that is, of higher (or lower) nodal value, obtained on the grid Ω^h to calculate the polynomial of degree p (ξ_p). Since ξ_p represents a convex function, the existence and uniqueness of its point of maximum (or minimum) in the interval set by such points are guaranteed. After obtaining the point of maximum (or minimum) (ϕ_{ext_i}), with $i = 1, \ldots, G$, for each grid Ω^h, we apply RRE with the Eq. (15), according to Algorithm 1.

Algorithm 1: Application of RRE in a variable with extreme values

Calculate ϕ, in different grids G: $\phi_1, \phi_2, \cdots, \phi_G$.
Obtain ξ_p, applying the polynomial interpolation.
Calculate the point of maximum or minimum (ϕ_{ext_i}) of ξ_p, for each grid Ω^h, $i = 1, \ldots, G$.
for $i = 1 : G$ **do**
  $\phi_{i,0} = \phi_{ext_i}$.
end for
for $m = 1 : G - 1$ **do**
  for $g = m + 1 : G$ **do**

$$\phi_{g,m} = \phi_{g,m-1} + \frac{\phi_{g,m-1} - \phi_{g-1,m-1}}{r^{p_{m-1}} - 1}.$$

  end for
end for

5 Results

We present the results obtained with the use of RRE, based on the methodology described in Sect. 3.2, which entailed the reduction and estimation of the numerical error for variables with extreme values for the one-dimensional poroelasticity problem.

We performed a computational code in Fortran language and Intel® Parallel Studio XE 2019 compiler. The machine had an Intel ® Core™ i7-9700KF processor, CPU 3.60 GHz and 16 GB of RAM. In all simulations, we considered quadruple precision and stop criterion, which is given by the dimensionless residual until the rounding error is reached. We used multigrid method with the following algorithmic components: CS scheme, standard coarsening ratio, $r = 2$, W(1,1)-cycle, Vanka smoother, full-weight restriction operator, and linear interpolation for prolongation. The coarsest grid that we considered was $N = 9$ nodal points and the finest with 8193 nodal points, in a total of $G = 11$ grids. We fixed $M = N + 1$ nodes for the spatial grid. We carried out two types of simulations with different values for Young's modulus E and hydraulic conductivity K, as follows.

Table 1 Input parameter for first poroelastic problem

Symbol	Quantity	Value	Unit
Ω	Spatial domain	$\left(0, \frac{1}{2}\right)$	m
T	Final time	1	s
E	Young's modulus	1	N/m^2
K	Hydraulic conductivity	1	m/s

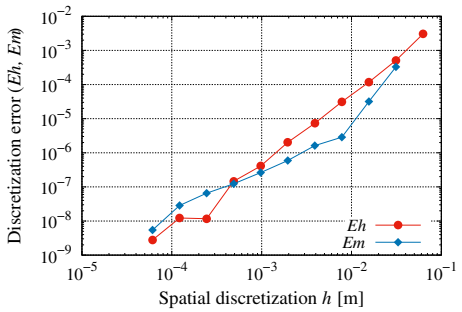

(a) Variable u_{max}.

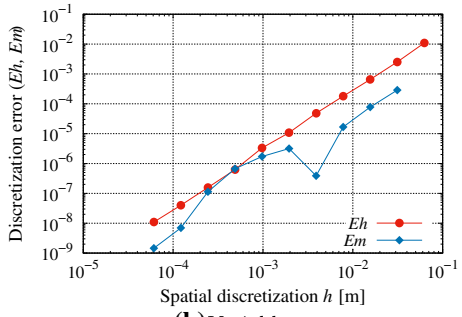

(b) Variable p_{max}.

Fig. 2 Discretization error without RRE (Eh) and with RRE (Em) *versus* spatial discretization (h)

5.1 Results for first poroelastic problem

First, we considered as variables of interest the maximum displacement value ($u_{\max}$) and the maximum pressure value ($p_{\max}$). With the nodal ϕ computed (maximum discrete

Table 2 Effective (pE) and apparent (pU) orders for the variables $u_{\max}$ and $p_{\max}$

grid	pE ($p_{\max}$)	pU ($p_{\max}$)	pE ($u_{\max}$)	pU ($u_{\max}$)
3.1×10^{-2}	2.11885		2.56950	
1.5×10^{-2}	1.94579	2.17492	2.11840	2.68099
7.8×10^{-3}	1.86095	1.97675	1.91413	2.18560
3.9×10^{-3}	1.89294	1.84899	2.09497	1.85402
1.9×10^{-3}	2.16675	1.80385	1.85251	2.17800
9.7×10^{-4}	1.69965	2.33414	2.30091	1.71199
4.8×10^{-4}	2.40988	1.46953	1.48817	2.60958
2.4×10^{-4}	1.99183	2.52690	3.64488	0.97247
1.2×10^{-4}	1.96780	1.99999	– 0.06362	7.99574
6.1×10^{-5}	1.87795	1.99999	2.13685	– 4.16253

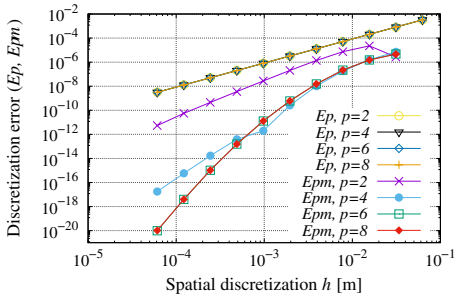

(a) Variable u_{max}.

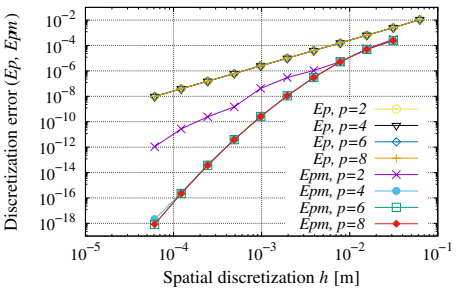

(b) Variable p_{max}.

Fig. 3 Discretization error for polynomial interpolation without the application of RRE (Ep) and with RRE (Epm) for $p = 2, 4, 6, 8$ *versus* spatial discretization (h)

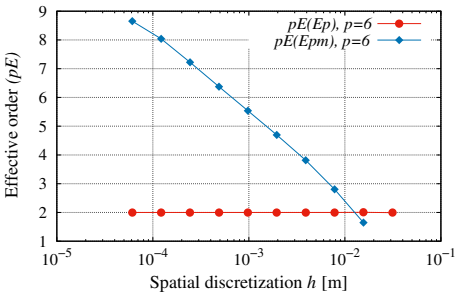

Fig. 4 Effective order with RRE pE (Ep) and without RRE pE (Epm) for the variable $u_{\max}$ *versus* spatial discretization (h)

Table 3 Effective pE and apparent pU orders for the variables $u_{\max}$ (with polynomial interpolation $p = 6$) and $p_{\max}$ (with polynomial interpolation $p = 4$)

grid	pE ($p_{\max}$)	pU ($p_{\max}$)	pE ($u_{\max}$)	pU ($u_{\max}$)
3.1×10^{-2}	1.99374		2.10356	
1.5×10^{-2}	2.00385	1.99036	1.97848	2.14373
7.8×10^{-3}	1.99992	2.00516	1.99978	1.97130
3.9×10^{-3}	2.00002	1.99989	1.99962	1.99983
1.9×10^{-3}	2.00000	2.00003	1.99991	1.99952
9.7×10^{-4}	2.00000	2.00000	1.99997	1.99989
4.8×10^{-4}	2.00000	2.00000	1.99999	1.99997
2.4×10^{-4}	2.00000	2.00000	1.99999	1.99999
1.2×10^{-4}	2.00000	2.00000	1.99999	1.99999
6.1×10^{-5}	2.00000	2.00000	1.99999	1.99999

Table 4 Effectiveness of the estimators $U_\Delta, U_{\text{cpm}}, U_\psi$ and U_{ψ^*}, for Epm, $p = 6$ and variable $u_{\max}$

grid	U_Δ/Epm	U_{cpm}/Epm	U_ψ/Epm	U_{ψ^*}/Epm
3.1×10^{-2}	689.43565	1.31929		1.31921
1.5×10^{-2}	4.13193	1.14304	− 7.92195	0.89535
7.8×10^{-3}	7.99094	1.07098	1.73156	0.94440
3.9×10^{-3}	15.08798	1.03859	1.78317	0.97170
1.9×10^{-3}	26.90764	1.02151	1.73293	0.98415
9.7×10^{-4}	47.46960	1.01206	1.73621	0.99093
4.8×10^{-4}	83.91856	1.00669	1.75180	0.99476
2.4×10^{-4}	150.29535	1.00380	1.78159	0.99714
1.2×10^{-4}	263.97815	1.00248	1.75137	0.99868

Table 5 Effectiveness of the estimators $U_\Delta, U_{\text{cpm}}, U_\psi$ and U_{ψ^*}, for Epm, $p = 4$ and variable $p_{\max}$

grid	U_Δ/Epm	U_{cpm}/Epm	U_ψ/Epm	U_{ψ^*}/Epm
3.1×10^{-2}	44.31086	1.20055		1.16888
1.5×10^{-2}	5.98623	1.10425	0.15791	0.93227
7.8×10^{-3}	10.59227	1.05790	1.64960	0.96184
3.9×10^{-3}	18.26886	1.03657	1.65892	0.98091
1.9×10^{-3}	28.33973	1.02372	1.52166	0.98803
9.7×10^{-4}	43.14445	1.01568	1.50418	0.99232
4.8×10^{-4}	64.74922	1.01062	1.48923	0.99509
2.4×10^{-4}	95.13034	1.00580	1.46200	0.99528
1.2×10^{-4}	173.14255	0.99176	1.81147	0.98612

value), we applied RRE. The input parameters for the first poroelastic problem are listed in Table 1. These values of E and K were used because they are typical values and are advantageous to show the effectiveness of the adopted methodology. Additionally, those parameters emphasize the influence of all the components of the model.

We noticed that the application of RRE to maximum discrete value has not presented a significant reduction in the error of the numerical solution with RRE applied (Em), in relation to Eh, according to the methodology proposed in Eq. 15, (Fig. 2a and b).

This inefficient effect might be explained by the changes in the coordinates of ϕ in different grids, which led to a non-asymptotic behavior of pE and pU when $h \to 0$, Table 2, thus hindering the performance of the RRE.

Then we followed the methodology presented in the Algorithm 1. That means to apply polynomial interpolation of degree p, then use the optimization method to calculate the maximum (or minimum) of the polynomial ξ_p , and

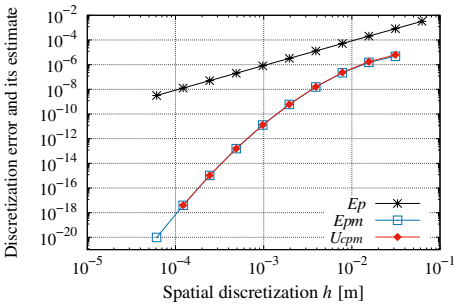

(a) Variable u_{max} $(p = 6)$.

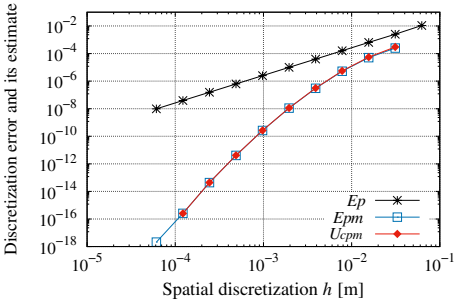

(b) Variable p_{max} $(p = 4)$.

Fig. 5 Discretization error for polynomial interpolation without the application of RRE (Ep), with RRE (Epm) and its estimate (U_{cpm}) *versus* spatial discretization (h)

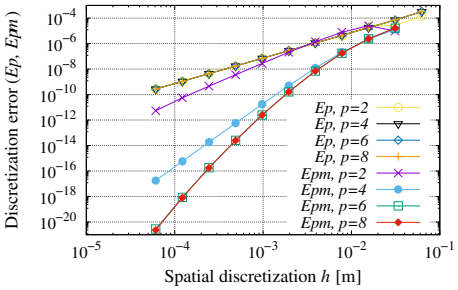

(a) Variable u_{max}.

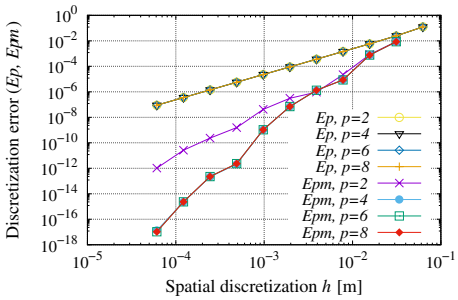

(b) Variable p_{max}.

Fig. 6 Discretization error for polynomial interpolation without the application of RRE (Ep) and with RRE (Epm) for $p = 2, 4, 6, 8$ *versus* spatial discretization (h)

Table 6 Input parameter for the second poroelastic problem

Symbol	Quantity	Value	Unit
Ω	Spatial domain	$\left(0, \frac{1}{2}\right)$	m
T	Final time	1	s
E	Young's modulus	10^2	N/m^2
K	Hydraulic conductivity	10^{-2}	m/s

therefore apply RRE. Figure 3a and b show the results for the numerical error after polynomial interpolation without the application of RRE (Ep) and with RRE (Epm).

With the refinement of the grid and the progressive increase of p, the discretization error Epm tends to zero more rapidly, Fig. 3, which evidences the efficiency of the methodology under analysis. We observed, however, that there is a limit for the increase of p, that is, for $p = 6$ or $p = 8$, the results are practically equivalent. This behavior is similar for higher values of p, for instance, $p = 10$. It must be highlighted that the non-asymptotic behavior of pE and pU when $h \to 0$, showed in Table 2, was smoothed as described in Table 3. Thus, the application of RRE presents behavior that is compatible with correlated theory, that is, a significant reduction of the discretization error.

Table 7 Effectiveness of the estimators $U_{\Delta}, U_{\text{cpm}}, U_{\psi}$ and U_{ψ^*}, for Epm, $p = 6$ and variable u_{max}

grid	U_{Δ}/Epm	U_{cpm}/Epm	U_{ψ}/Epm	U_{ψ^*}/Epm
3.1×10^{-2}	21.69207	1.14796		1.09026
1.5×10^{-2}	7.75847	1.07310	0.38994	0.94271
7.8×10^{-3}	14.67994	1.03992	1.78371	0.97113
3.9×10^{-3}	26.04447	1.02349	1.72294	0.98479
1.9×10^{-3}	43.56666	1.01520	1.64734	0.99208
9.7×10^{-4}	66.77492	1.01036	1.52057	0.99530
4.8×10^{-4}	97.48064	1.00702	1.45298	0.99672
2.4×10^{-4}	143.41285	1.00470	1.46637	0.99771
1.2×10^{-4}	213.68982	1.00330	1.48662	0.99862

In Table 3, we verify that with the refinement of the grid, the effective pE and apparent pU orders of Ep asymptotically converge to 2, in accordance with what is described in [39]. Also, in Fig. 4, we can notice that the use of RRE generated a progressive increase in the accuracy order $(\text{pE})_{g,m}$, resulting in the maximum value of 8.654 for u_{max}.

In order to choose the most appropriate error estimator, we calculated their effectiveness θ. Tables 4 and 5 show the values of θ for the estimators $U_{\Delta}, U_{\text{cpm}}, U_{\psi}$ and U_{ψ^*} for the variables u_{max} and p_{max}, respectively.

Table 8 Effectiveness of the estimators $U_\Delta, U_{\text{cpm}}, U_\psi$ and U_{ψ^*}, for Epm, $p = 6$ and variable $p_{\max}$

grid	U_Δ/Epm	U_{cpm}/Epm	U_ψ/Epm	U_{ψ^*}/Epm
3.1×10^{-2}	15.59520	1.08998		1.01878
1.5×10^{-2}	12.11291	1.01115	0.791294	0.93324
7.8×10^{-3}	90.65773	0.84486	0.698479	0.83706
3.9×10^{-3}	5.44615	1.05254	− 0.502859	1.30468
1.9×10^{-3}	20.03297	1.01522	− 0.479912	0.96625
9.7×10^{-4}	66.69933	0.99799	0.321712	0.98328
4.8×10^{-4}	498.78575	1.10243	− 0.735313	1.10487
2.4×10^{-4}	10.76208	1.01058	− 0.238395	0.92383
1.2×10^{-4}	95.49441	1.00579	8.197380	0.99530

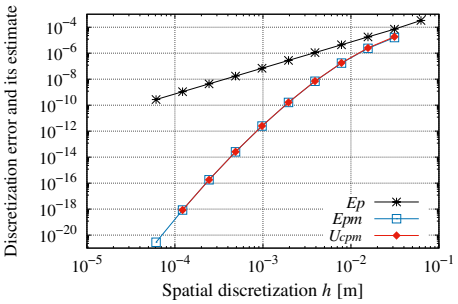

(a) Variable u_{max} $(p = 6)$.

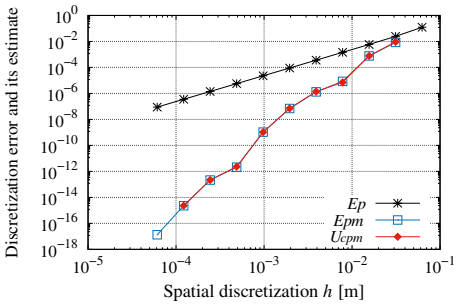

(b) Variable p_{max} $(p = 4)$.

Fig. 7 Discretization error for polynomial interpolation without the application of RRE (Ep), with RRE (Epm) and its estimate (U_{cpm}) *versus* spatial discretization (h)

Notice that the more accurate estimates for the discretization error are established by U_{cpm} and U_{ψ^*}, that is, with ratios $\frac{U_{\text{cpm}}}{\text{Ep}} \approx 1$ and $\frac{U_{\psi^*}}{\text{Ep}} \approx 1$. With regard to reliability, U_{cpm} shows to be reliable for $u_{\max}$, it has a ratio $\frac{U_{\text{cpm}}}{\text{Em}} > 1$. For the variable $p_{\max}$, the estimator U_{cpm} could not be considered reliable only for grid $h = 1.2 \times 10^{-4}$. Figure 5 shows the results for Epm and its estimate U_{cpm}.

The effect of RRE in the reduction of Ep can be measured by the calculation of the ratio |Ep|/|Epm|. For instance, for the variable $u_{\max}$ and for the grid $h = 9.7 \times 10^{-4}$, the use of RRE (with 6 levels of extrapolation) reduced the discretization error in 6.2×10^4, that is, the error was reduced more than 62 thousand times.

5.2 Results for the second poroelastic problem

We obtained the solutions $\phi = u_{\max}$ and $\phi = p_{\max}$ with the mathematical model presented in Sect. 2. The input parameters for the second poroelastic problem are listed in Table 6.

These values of E and K were assigned with the purpose of presenting a poroelastic problem where the terms of Eq. (1) do not present equal weights and then perform a numerical verification of the solutions obtained against the RRE applied to variables with extreme values. The hydraulic conductivity $K = 10^{-2}$ m/s represents the physical problem for a soil composed of clean gravel, [4, 16] (realistic problem). Figure 6 show the results for Ep and Epm with $p = 2, 4, 6$ and 8.

The results obtained are similar to those exposed previously for the reduction of the numerical error. The values for effectiveness θ, for the estimators $U_\Delta, U_{\text{cpm}}, U_\psi$ and U_{ψ^*} the variables $u_{\max}$ and $p_{\max}$ are presented in Tables 7 and 8.

The estimators that resulted more accuracy were U_{cpm} and U_{ψ^*}, that is, $\frac{U_{\text{cpm}}}{\text{Ep}} \approx 1$ and $\frac{U_{\psi^*}}{\text{Ep}} \approx 1$. Table 7 shows that among these estimators, only U_{cpm} proved to be reliable. However, for the variable $p_{\max}$, Table 8, grids $h = 7.8 \times 10^{-3}$ and $h = 9.7 \times 10^{-4}$, the estimator U_{cpm} showed a ratio $\frac{U_{\text{cpm}}}{\text{Em}} < 1$, indicating that it is not reliable for these two grids. Figure 7a and b present the results for the discretization error Epm and its estimate U_{cpm}.

As one example, the evaluation of the ratio |Ep|/|Epm|, for the grid $h = 4.8 \times 10^{-4}$ (with 7 levels of extrapolation) shows a reduction of the discretization error for the variable $u_{\max}$ of 6.7×10^5, that is, a reduction of more than 670 thousand times.

6 Conclusion

In this work, we evaluated the effectiveness of using Repeated Richardson extrapolation (RRE) for a problem of one-dimensional poroelasticity for variables with extreme values aiming to reduce the discretization error and increase the accuracy of the numerical solution. We concluded that: (1) the direct application of RRE to variables with extreme values does not lead to a significant reduction of Eh; (2) the previous application of polynomial interpolation to variables with extreme values followed by the use of an optimization method resulted in a considerable reduction of Eh; (3) the use of RRE, based on the adopted methodology, provided a significant progressive increase in the order of accuracy of numerical solutions; (4) with regard to the estimates of the

numerical error, considering the solutions obtained with the application of RRE, the Corrected Richardson's estimator (U_{cpm}) is recommended for providing better accuracy and reliability than the others that we tested in this work.

Acknowledgements The first author would like to thank the State University of Centro-Oeste (UNICENTRO) for the financial grant and the full-time license to PhD studies. The authors thank the Graduate Program in Numerical Methods in Engineering of the Federal University of Parana (UFPR)

References

1. AbdelMigid TA, Saqr KM, Kotb MA, Aboelfarag AA (2017) Revisiting the lid-driven cavity flow problem: review and new steady state benchmarking results using gpu accelerated code. Alex Eng J 56(1):123–135. https://doi.org/10.1016/j.aej.2016.09.013
2. Alpak F, Wheeler M (2012) A supercoarsening multigrid method for poroelasticity in 3D coupled flow and geomechanics modeling. Comput Geosci 16:953–974. https://doi.org/10.1007/s10596-012-9297-z
3. Bank RE, Dupont TF, Yserentant H (1988) The hierarchical basis multigrid method. Numer Math 52:427–458. https://doi.org/10.1007/BF01462238
4. Bear J (1972) Dynamics of fluids in porous media. Dover Publications, New York, NY, USA
5. Biot MA (1941) General theory of three dimensional consolidation. J Appl Phys 12:155–164. https://doi.org/10.1063/1.1712886
6. Biot MA (1955) Theory of elasticity and consolidation for a porous anisotropic solid. J Appl Phys 26:182–185. https://doi.org/10.1063/1.1721956
7. Briggs WL, Henson VE, McCormick SF (2000) A multigrid tutorial, 2nd edn. SIAM, Philadelphia
8. Chapra SC, Canale RP (1994) Introduction to computing for engineers, 2nd edn. McGraw-Hill College, New York
9. Dahlquist G, Bjorck A (2008) Numerical methods in scientific computing. SIAM, Philadelphia
10. Ehlers W, Bluhm J (2002) Porous media: theory. Experiments and Numerical Applications, Springer, Berlin, Germany
11. Ertuk E, Corke TC, Gokçol C (2005) Numerical solutions of 2-D steady incompressible driven cavity flow at high reynolds numbers. Int J Numer Meth Fluids 48:747–774. https://doi.org/10.1002/fld.953
12. Fedorenko R (1964) The speed of convergence of one iterative process. USSR Comput Math Math Phys 4(3):227–235. https://doi.org/10.1016/0041-5553(64)90253-8
13. Ferziger JH, Perić M (2002) Computational methods for fluid dynamics, 3rd edn. Springer, New York
14. Franco SR, Gaspar FJ, Pinto MAV, Rodrigo C (2018) Multigrid method based on a space-time approach with standard coarsening for parabolic problems. Appl Math Comput 317:25–34. https://doi.org/10.1016/j.amc.2017.08.043
15. Franco SR, Rodrigo C, Gaspar FJ, Pinto MAV (2018) A multigrid waveform relaxation method for solving the poroelasticity equations. Comp Appl Math 37:4805–4820. https://doi.org/10.1007/s40314-018-0603-9
16. Freeze RA, Cherry JA (1979) Groundwater. Prentice-Hall. Inc., London
17. Gaspar FJ, Lisbona FJ, Osterlee CW (2008) A stabilized difference scheme for deformable porous media and its numerical resolution by multigrid methods. Comput Vis Sci 11:67–76. https://doi.org/10.1007/s00791-007-0061-1
18. Gaspar FJ, Lisbona FJ, Osterlee CW, Vabishchevich PN (2007) An efficient multigrid solver for a reformulated version of the poroelasticity system. Comput Methods Appl Mech Eng 196:1447–1457. https://doi.org/10.1016/j.cma.2006.03.020
19. Gaspar FJ, Lisbona FJ, Vabishchevich PN (2003) A finite difference analysis of Biot's consolidation model. Appl Numer Math 44:487–506. https://doi.org/10.1016/S0168-9274(02)00190-3
20. Gaspar FJ, Lisbona FJ, Vabishchevich PN (2006) Staggered grid discretizations for the quasi-static Biot's consolidation problem. Appl Numer Math 56:888–898. https://doi.org/10.1016/j.apnum.2005.07.002
21. Guo J, Chang L (2020) Repeated richardson extrapolation and static hedging of barrier options under the cev model. J Futur Mark 40(6):974–988. https://doi.org/10.1002/fut.22100
22. Li M, Zheng Z, Pan K, Yue X (2020) An efficient Newton multiscale multigrid method for 2D semilinear Poisson equations. East Asian J Appl Math 10(3):620–634. https://doi.org/10.4208/eajam.090120.260320
23. Luo P, Rodrigo C, Gaspar FJ (2015) Multigrid method for nonlinear poroelasticity equations. Comput Vis Sci 17:255–265. https://doi.org/10.1007/s00791-016-0260-8
24. Malacarne MF, Pinto MAV, Franco SR (2021) Performance of the multigrid method with time-stepping to solve 1d and 2d wave equations. Int J Comput Methods Eng Sci Mech 1:1–12. https://doi.org/10.1080/15502287.2021.1910750
25. Marchi CH, Araki LK, Alves AC, Suero R, Gonçalves SFT, Pinto MAV (2013) Repeated richardson extrapolation applied to the two-dimensional laplace equation using triangular and square grids. Appl Math Model 37:4661–4675. https://doi.org/10.1016/j.apm.2012.09.071
26. Marchi CH, Germer EM (2013) Effect of ten cfd numerical schemes on repeated richardson extrapolation (rre). J Appl Comput Math 2(128):1–8. https://doi.org/10.4172/2168-9679.1000128
27. Marchi CH, Martins MA, Novak LA, Araki LK, Pinto MAV, Gonçalves SFT, Moro DF, Freitas IS (2016) Polynomial interpolation with repeated richardson extrapolation to reduce discretization error in CFD. Appl Math Model 40:8872–8885. https://doi.org/10.1016/j.apm.2016.05.029
28. Marchi CH, Novak LA, Santiago CD, Vargas APS (2013) Highly accurate numerical solutions with repeated richardson extrapolation for 2D laplace equation. Appl Math Model 37:7386–7397. https://doi.org/10.1016/j.apm.2013.02.043
29. Marchi CH, Silva AFC (2002) Unidimensional numerical solution error estimation for convergent apparent order. Numer Heat Transf Part B 42:167–188. https://doi.org/10.1080/10407790190053888
30. Marchi CH, Suero R, Araki LK (2009) The lid-driven square cavity flow: numerical solution with a 1024 x 1024 grid. J Br Soc Mech Sci Eng 31(3):186–198. https://doi.org/10.1590/S1678-58782009000300004
31. Nicolas X, Medale M, Glockner S, Gounand S (2011) Benchmark solution for a three-dimensional mixed-convection flow, part 1: Reference solutions. Numer Heat Transf Part B Fundam 60(5):325–345. https://doi.org/10.1080/10407790.2011.616758
32. Oliveira F, Franco SR, Pinto MAV (2018) The effect of multigrid parameters in a 3d heat diffusion equation. Int J Appl Mech Eng 23:213–221. https://doi.org/10.1515/ijame-2018-0012
33. Pinto MAV, Rodrigo C, Gaspar FJ, Oosterlee C (2016) On the robustness of ILU smoothers on triangular grids. Appl Numer Math 106:37–52. https://doi.org/10.1016/j.apnum.2016.02.007
34. Rahul K, Bhattacharyya SN (2006) One-sided finite-difference approximations suitable for use with richardson extrapolation. J Comput Phys 219:13–20. https://doi.org/10.1016/j.jcp.2006.05.035
35. Richardson LF, Gaunt JA (1927) The deferred approach to the limit. Philos Proc Roy Soc Lond 226:299–361. https://doi.org/10.1098/rsta.1927.0008

36. Rodrigues S, Pinto MAV, Franco SR, Martins MA (2020) Reducing the discretization error for global and local variables in poroelasticity problems. In: Proceedings of the Ibero-Latin-American congress on computational methods in engineering, pp 1–7. https://cilamce.com.br/anais/index.php?ano=2020
37. Roy JC (2005) Review of code and solution verification procedures for computational simulation. J Comput Phys 205:131–156. https://doi.org/10.1016/j.jcp.2004.10.036
38. Roy JC, Obeekampf WL (2011) A comprehensive framework for verification, validation, and uncertainty quantification in scientific computing. Comp Meth Appl Mech Eng 200:2131–2144. https://doi.org/10.1016/j.cma.2011.03.016
39. Strikwerda JC (2004) Finite difference schemes and partial differential equations, 2nd edn. Society for Industrial and Applied Mathematics
40. Trottenberg U, Oosterlee C, Schüller A (2001) Multigrid. Academic Press, San Diego
41. Vanka S (1986) Block-implicit multigrid solution of navier-stokes equations in primitive variables. J Comput Phys 65(1):138–158. https://doi.org/10.1016/0021-9991(86)90008-2
42. Wesseling P (1992) An introduction to multigrid methods. John Wiley & Sons, Chichester
43. Wienands R, Gaspar FJ, Lisbona FJ, Osterlee CW (2004) An efficient multigrid solver based on distributive smoothing for poroelasticity equations. Computing 73:99–119. https://doi.org/10.1007/s00607-004-0078-y
44. Zhu JZ, Zienkiewicz OC (1990) Superconvergence recovery technique and a posteriori error estimators. Int J Numer Meth Eng 30:1321–1339. https://doi.org/10.1002/nme.1620300707